

# In Vitro, In Silico, and In Vivo Studies of *Cardamine hirsuta* Linn as a Potential Antidiabetic Agent in a Rat Model

Published as part of the ACS Omega virtual special issue "Phytochemistry".

Aqna Malik, Ali Sharif,\* Hafiz Muhammad Zubair, Bushra Akhtar, and Aisha Mobashar



Cite This: *ACS Omega* 2023, 8, 22623–22636



Read Online

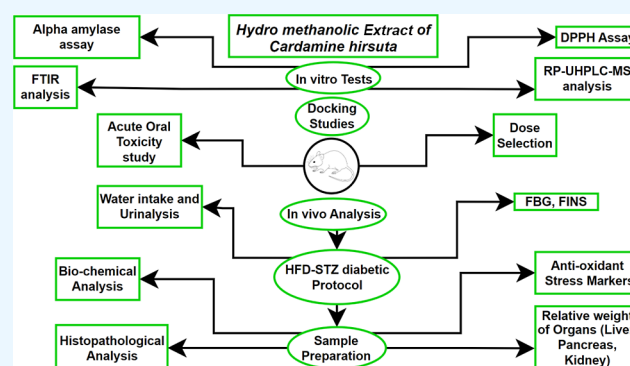
ACCESS |

Metrics & More

Article Recommendations

Supporting Information

**ABSTRACT:** Diabetes mellitus (T2DM) is a multifaceted metabolic disorder with no definite treatment. In silico characterization can help to explain the interaction between molecules and predict 3D structures. The aim of the present study was to evaluate the hypoglycemic activities of the hydro-methanolic extract of *Cardamine hirsuta* in a rat model. In vitro antioxidant and  $\alpha$ -amylase inhibitory assays were evaluated in the present study. Phytoconstituents were quantified using RP-UHPLC-MS analysis. Molecular docking of compounds into the binding site of different molecular targets, i.e., tumor necrosis factor (TNF- $\alpha$ ), glycogen synthase kinase 3  $\beta$  (GSK-3 $\beta$ ), and AKT, was carried out. Acute toxicity model, in vivo antidiabetic effect, and the influence on biochemical and oxidative stress parameters were also investigated. T2DM was induced in adult male rats by streptozotocin using a high-fat diet model. Three different doses (125, 250, and 500 mg/kg BW) were orally gavaged for 30 days. Mulberrofuran-M and quercetin3-(6''caffeoylsophoroside) have demonstrated remarkable binding affinity toward TNF- $\alpha$  and GSK-3 $\beta$ , respectively. 2,2-Diphenyl-1-picrylhydrazyl and  $\alpha$ -amylase inhibition assay exhibited IC<sub>50</sub> values of 75.96 and 73.66  $\mu$ g/mL, respectively. In vivo findings exhibited that 500 mg/kg body weight (BW) dose of the extract significantly decreased the blood glucose level, improved biochemical parameters as well as oxidative stress by reduction of lipid peroxidation, and increased high-density lipoproteins. Moreover, activities of glutathione-s-transferase, reduced glutathione, superoxide dismutase were enhanced, and cellular architecture in the histopathological examination was restored in treatment groups. The present study affirmed the antidiabetic activities of mulberrofuran-M and quercetin3-(6''caffeoylsophoroside) present in the hydro-methanolic extract of *C. hirsuta*, possibly due to the reduction in oxidative stress and  $\alpha$ -amylase inhibition.



## 1. INTRODUCTION

Type 2 DM is a complicated metabolic disorder of elevated blood glucose levels. The toll of diabetic individuals has risen to 422 million in the last 2 decades.<sup>1</sup> Similarly, the incidence of diabetes in young adults over 18 also increased from 4.7 to 8.5%.<sup>2</sup> High prevalence is noted in underdeveloped countries or low-income populations than higher class due to less awareness about healthy life style and high intake of carbohydrates diet. Chronic diabetic complications are neuropathy, nephropathy, and cardiac problems worldwide.<sup>3</sup>

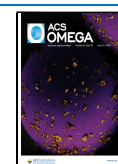
Impaired glucose tolerance spurred on by insulin resistance linked with  $\beta$ -islet cell degeneration which is the main reason for type 2 DM leading to insulin deficiency, utilization of glucose in skeletal muscle, liver, and adipose tissues.<sup>4</sup> Genetic predisposition, environmental factor, diet, physical inactivity, and obesity are key factors which play a role in impaired glucose tolerance leading to insulin resistance and type 2 DM. Reactive oxygen species (ROS) contribute in the development of type 2 DM due to free radicals, hyperglycemic oxidation. Oxidative stress, non-enzymatic protein glycation, and

increased lipid peroxidation result in free radicals (FFAs) production to further degrade enzymes and cellular apparatus resulting in the insulin resistance.<sup>5</sup> Hyperglycemia disturbs the lipid profile and renders cells more prone to lipid peroxidation. Systemic inflammation is mainly responsible for pathological changes during diabetic complications (both macro and micro) which are mainly worsened by oxidative stress. These diabetic complications include coronary artery disease, neuropathy, nephropathy, retinopathy, and stroke. Hence, DM can be elucidated mainly by an increase in vascular disease other than hyperglycemia.<sup>6</sup>

Received: February 24, 2023

Accepted: May 30, 2023

Published: June 12, 2023



Conventional DM medications have many unwanted side effects including nausea, diarrhea, hypoglycemia, weight gain, hypersensitivity, GIT disturbances, heart and liver failure, and weight gain. Glucose metabolism in diabetics has reportedly been improved due to herbal remedies, diet plans, alternative, and complementary therapies. Numerous plant extracts have been shown to be effective in maintaining glucose homeostasis in recent clinical investigations. The regulation of carbohydrate metabolism is aided by herbal products containing high levels of flavonoids, phenolic compounds, terpenoids, alkaloids, glycosides, and coumarins. Despite being superior to the current drug system in terms of effectiveness, traditional medicine has significant challenges due to the absence of sufficient standards.<sup>7</sup>

*Cardamine hirsuta* Linn is a winter annual or biennial member of the Cardamine genus that belongs to the Brassicaceae family which can reach up to 30 cm (113/4 in.) in height. The native range of *C. hirsuta* is the Northern Hemisphere to tropical African mountains and is widespread all over the world. *C. hirsuta* grows in moist, muddy places and can be found in various areas of Pakistan like Batkhela, Abbottabad, Swat (KPK), Gilgit, Chitral, and Kashmir (flora of Pakistan). Traditional names of *C. hirsuta* are hairy bittercress, lambs' cress, land cress, spring cress, hoary bittercress, shot weed, and flick weed. It has a strong antioxidant potential.<sup>8</sup>

In silico approaches have been used to tackle a number of biological problems by explaining the interaction of molecules and predicting 3D structures. Main objective of the study was to estimate the blood glucose lowering and antioxidant effects of *C. hirsuta* (CH) extract on diabetic complications. These may include oxidative damage and hyperlipidemia in high-fat diet (HFD)/streptozotocin (STZ)-induced type 2 diabetic Sprague-Dawley (SD) rats. It will also perform an in silico analysis of the compounds discovered using RP-UHPLC-MS. To the best of our knowledge, little is known about effects of *Cardamine Hiruta* on Type-2 DM and related complications.

## 2. MATERIALS AND METHODS

**2.1. Plant Material.** *C. hirsuta* L. whole plant was collected in January 2018 from Batkhela, Pakistan and authentication was confirmed by the Department of Botany, Government College University, Lahore (GCUL), received voucher # 3444. The shade-dried whole plant was powdered and hydro-methanolic (10:90) extract was prepared by maceration. The filtrate was concentrated under reduced pressure using a rotary evaporator (RV10B S99, IKA). The final filtrate was kept in a desiccator and then transferred to a pre-weighed Petri plate. The final yield was calculated according to following formula.

$$\text{percentage yeild \%} = \frac{\text{actual yeild}}{\text{theoratical yeild}} \times 100$$

Above was kept at 20 °C for further uses.<sup>9</sup> Hydro-methanolic extract of *C. hirsuta* was examined for phytochemical analysis.

**2.2. In Vitro Antioxidant 2,2-Diphenyl-1-picrylhydrazyl Assay.** The antioxidant activity of hydro-methanolic extract of *C. hirsuta* was estimated by 2,2-diphenyl-1-picrylhydrazyl (DPPH) scavenging assay with some modifications. Ascorbic acid was used as the standard. 2 mL of freshly prepared DPPH solution was added to 1 mL of extract and incubated for 30 min. The absorbance was recorded by a UV spectrophotometer at 517 nm. IC<sub>50</sub> was calculated using

percentage inhibitions at different concentrations of the extract.<sup>10,11</sup>

$$\text{inhibition \%} = \left[ \frac{\text{absorbance (control)} - \text{absorbance (sample)}}{\text{absorbance (control)}} \right] \times 100$$

**2.3. Alpha-Amylase Inhibitory Assay.** Hypoglycemic potential of hydro-methanolic extract of *C. hirsuta* was evaluated via the  $\alpha$ -amylase inhibition assay by following the standard protocol<sup>12</sup> Acarbose was used as the positive control, whereas negative control or blank were prepared without sample only and without sample and amylase enzyme. Absorbance was noted at  $\lambda$ 540 nm and the inhibitory potential of  $\alpha$ -amylase enzyme was calculated using the following formula.

$$\% \alpha \text{ amylase inhibition} = \frac{\text{absorbance of control} - \text{absorbance of sample}}{\text{absorbance of control}} \times 100$$

To determine the inhibitory concentration (IC<sub>50</sub>), %  $\alpha$ -amylase inhibition for each sample was plotted against the log of the sample concentration.

**2.4. Fourier-Transform Infrared Spectroscopy Analysis.** Defatted hydro-methanolic extract of *C. hirsuta* was analyzed using Fourier-transform infrared (FTIR) spectroscopy (Agilent technologies) at  $\lambda$ 7600 (KBr) pellet method in a transmittance mode (4000–650 cm<sup>-1</sup>).<sup>13</sup>

**2.5. Reversed-Phase Ultra-High Performance Liquid Chromatography Analysis.** Reversed-phase ultrahigh-performance liquid chromatography (RP-UHPLC) coupled to diode array detection (DAD) and mass spectrometry (MS) was used for secondary metabolites profiling of defatted hydro-methanolic extract of *C. hirsuta* by an Agilent 1290 Infinity LC system coupled to an Agilent 6520 Accurate-Mass Q-TOF mass spectrometer with a dual ESI source.<sup>14</sup>

**2.6. Structure Prediction.** 3 targeted RAT proteins, tumor necrosis factor (TNF) (235 amino acids), GSK-3 (420 amino acids), and AKT-1 (480 amino acids), had their amino acid residues extracted in the FASTA format from the UniProt knowledge base database. Using BLASTp to find templates for the PDB IDs P16599, P49841, and P47196, respectively, amino acid sequences were compared. By satisfying the spatial constraints, an automated protein modeling application called Swiss modeling and Modeller-v.9.20 were used to predict the 3D structures of all targeted proteins. Approach to threading (ESyPred3D),<sup>15</sup> 3D-JigSaw,<sup>16</sup> I-TASSER,<sup>17</sup> and MOD-WEB<sup>18</sup> for structure prediction were also employed to predict the efficient 3D models.<sup>19</sup> Verify3D<sup>20</sup> and Rampage<sup>21</sup> were applied to evaluate the quality of the predicted 3D. Utilizing UCSF Chimera 1.12, the energy minimization and geometry optimization processes were carried out<sup>22</sup> using the conjugate gradient method for 1000 steps (step size 0.02), followed by protonation of wild-type histidines using the AMBER force field method.<sup>23</sup>

**2.7. Molecular Docking.** ChemDraw Ultra and UCSF Chimera 1.12 were utilized to determine the geometry optimization and energy minimization of the screened compounds. AutoDock Vina performed molecular docking research.<sup>24,25</sup> Polar hydrogen atoms were added to all of the targeted proteins, and the total number of docking runs was set

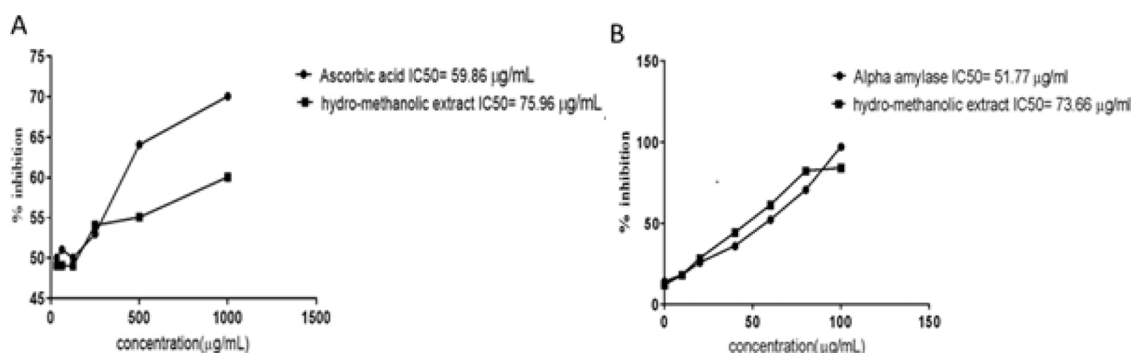


**Figure 1.** Antioxidant assays. Percentage inhibition of hydro-methanolic extract of *C. hirsuta* in DPPH assay (A). Percentage inhibition of hydro-methanolic extract of *C. hirsuta* in Alpha amylase assay (B). Data are presented as mean  $\pm$  SD,  $n = 3$ .

to 100 for each docking experiment. The tools from Discovery Studio,<sup>26</sup> UCSF Chimera 1.1, and AutoDock Vina were used to display and evaluate the docked complexes. The ADMET SAR server examined the ADMET characteristics.

**2.8. Animals and Ethical Statement.** 8-week male SD rats were purchased from the Post Graduate Medical Institute (PGMI), Lahore's animal house where they were raised in pathogen-free environments. All rats were housed in spacious, large-sized polyacrylic cages with a 12 h light/dark cycle and 70% humidity. Animal Ethics Committee at The University of Lahore, Pakistan, authorized the animal care procedure (IREC-2018-46).

**2.9. Acute Toxicity Test.** According to OECD Guideline 423, an oral acute toxicity test was performed. Five groups of healthy SD male rats ( $n = 6$ ) were selected. *C. hirsuta* hydro-methanolic extract was administered orally with 1% sodium carboxy methylcellulose (Na-CMC) at various dosages (50, 100, 500, 1000, and 2000 mg/kg BW).<sup>27</sup>

**2.10. Induction of Type 2 Diabetes Mellitus.** The experimental SD rats were fed HFD (45% fat) for 30 days to induce diabetes.<sup>28</sup> Later on, freshly prepared and diluted in 0.1 M of citrate buffer (pH 4.5), solution of streptozotocin (STZ) (55 mg/kg BW) was injected intraperitoneally. Diabetic rats were evaluated on the basis of blood glucose levels exceeding 200 mg/dL after 72 h of induction.<sup>29</sup> SD rats in the negative control group were fed a normal pellet diet.

**2.11. Experimental Design.** SD rats were casually separated into six groups ( $n = 5$  each) as follows:

Group 1: normal control rats (NC) received normal saline (1 mL/kg) orally

Group 2: HFD-STZ rats (diabetic control) diabetes induced by streptozotocin (STZ) (55 mg/kg, i.p) and was fed a HFD

Group 3: HFD-STD (positive control) diabetic rats received glibenclamide 600 μg/kg, PO

Group 4: HFD-STZ125, diabetic rats received hydro-methanolic extract of *C. hirsuta* 125 mg/kg, PO

Group 5: HFD-STZ 250 diabetic rats received hydro-methanolic extract of *C. hirsuta* 250 mg/kg, PO

Group 6: HFD-STZ 500, diabetic rats received hydro-methanolic extract of *C. hirsuta* 500 mg/kg, PO

Each experimental SD rat group utilized normal saline as the vehicle. Weekly record of water intake mL/day was kept.<sup>30</sup> Rats were anaesthetized with either at the end of the 60-day experimental period. Tissue and blood samples were taken for further examination. The internal organs (liver, kidney, and pancreas) were also weighed.

**2.12. Biochemical Analysis.** Accu-Check glucometer was used to check FBG from tail veins of each experimental rat after every 3 days during experimental study. Fasting insulin levels [FINS (IU/mL)] were also assessed at days 0, 7, 30, 35, and 60 days. SD rats were fasted overnight on day 61 of the experimental study. Blood samples, which were drawn via heart puncture and kept in sterile containers, were kept for 2 h at RT. Centrifugation was done for 15 min at 1500g at 4 °C. Triglycerides (TGs), total cholesterol (TC), high-density lipoprotein cholesterol (HDL-C), low-density lipoprotein cholesterol (LDL-C), aspartate aminotransferase (AST), alkaline phosphatase (ALP), alanine aminotransferase (ALT), urea, and creatinine were evaluated after separation of supernatant from the pellet soon after its formation. All blood samples were referred to UOL Diagnostic Lab and Research Center for analysis of biochemical parameters. Glycogen levels in the liver and skeletal muscles were also assessed via kits from Nanjing Jiancheng Bioengineering in accordance with manufacturer recommendations.

**2.13. Urine Analysis.** Urine analysis was also performed at day 0, 7, 30, 35, and 60 by taking fresh urine after 12 h fasting to check the level of urea and creatinine from all the experimental groups using Roche Cobas C111 Chemistry Analyzer Display Module Monitor #10325. Urine volume output was also measured.

**2.14. Oxidative Stress Biomarkers.** The anti-oxidant parameters malonaldehyde (MDA), total-antioxidant capacity (T-AOC), superoxide dismutase (SOD), catalase (CAT), glutathione peroxidase (GSH-PX), glutathione-S-transferase (GSH-ST), and glucose 6-phosphate dehydrogenase (G6PD) were measured using standardized kits. The kits were purchased from Nanjing Jiancheng Bioengineering Institute, China and manufacturer instructions were followed in carrying out the experiments. All the experiments were performed in triplicate.<sup>31</sup>

**2.15. Hematoxylin and Eosin (H&E) Staining.** Removal, dissection, and rinsing of internal organs (liver, kidney, and pancreas) from all HFD-STZ groups and NC group was done with an ice-cold saline solution following preservation in neutral formalin solution of 10%. After being cleaned, dehydrated with alcohol, and clarified with xylene, paraffin blocks were made and sections with a thickness of 4–5 mm were cut using a rotary microtome and stained with hematoxylin and eosin. Examination of slides were done under a light microscope for any signs of toxicity after treatment for histopathological alterations (optika vision lite 2.1).<sup>32</sup>

**2.16. Statistical Analysis.** Statistical analysis was performed using GraphPad Prism 9.0.2. Data are presented as the mean  $\pm$  SEM. The significance of the data was evaluated by a one-way ANOVA followed by a Tukey post hoc test was used to compare between groups. \*\*\* represent  $p < 0.001$  when compared to NC group, \*\* represent  $p < 0.01$  when compared to NC group, \* represent  $p < 0.05$  when compared to the NC group, ### represents  $p < 0.001$  when compared with HFD-STZ, ## represent  $p < 0.01$  when compared to HFD-STZ, and # represent  $p < 0.05$  when compared to HFD-STZ.

### 3. RESULTS

**3.1. Yield % and Qualitative Analysis.** The yield of hydro-methanolic extract of *C. hirsuta* was 6.26% (w/w) and it was stored in an amber-colored glass vials. Qualitative phytochemical analysis included the presence of alkaloids, steroids, flavonoids, and terpenoids in the extract.

**3.2. Antioxidant Capacity.** **3.2.1. In Vitro Antioxidant DPPH Assay.** Capacity of the crude extracts to scavenge free radicals was checked through the DPPH assay. DPPH free radicals absorb an electron from the antioxidants to undergo reduction and resulting in purple hue of the DPPH solution to yellow. The standard in the DPPH assay, ascorbic acid, exhibited the lowest IC<sub>50</sub> 59.86 g/mL with a 70.09% inhibition (Figure 1A). The hydro-methanolic extract of *C. hirsuta* had the greatest percentage inhibition at 1000 g/mL (60.08%) with an IC<sub>50</sub> of 75.96  $\mu$ g/mL.

**3.3. Alpha-Amylase Inhibitory Assay.** Concentration-dependent inhibition was exhibited by the hydro-methanolic extract of *C. hirsuta* which was highest at maximum dose 100  $\mu$ g/mL. The percentage inhibition of *C. hirsuta* was 97.23% (IC<sub>50</sub>–73.66  $\mu$ g/mL) as compared to that of Acarbose 51.77  $\mu$ g/mL (Figure 1B).

**3.4. FTIR Spectroscopy Analysis.** FTIR spectrum depicted different peaks (Table 1). The peak characteristics of alcohol are 1064/cm (C–O) stretch, 1094/cm (C–O) stretch, 1328/cm (H–O) stretch, phenol or tertiary alcohol, 1595/cm might be aromatic (C=C) bending, 1094/cm is amine (C–N) stretch, 1278/cm is aromatic amine (C–N) stretch, 1574/cm is amine (C–N) bending, 3132/cm is amine (N–H) stretch, and 3630/cm, 3567/cm, 3548/cm, and 3490/cm all are related to (O–H) alcohol in a different environments like intermolecular bonding. 2040/cm might be (N=C=S) isothiocyanate, 1399/cm is sulfoxide (S=O) stretch, 1507/cm is nitro (N–O) stretch, 1472/cm (C=C) may be attached with the methylene group, 890/cm, 991/cm (C=C) is olefinic functional group attached with different substituents (N–H) stretch, 2132/cm may be (S–C=N) thio-cyanide, 846/cm might be alkyl halide (C–Cl), 2570/cm (S–H) may be thiol, and 2398/cm may be (O=C=O) carbon dioxide from air. 2857/cm, 2909/cm, and 2948/cm all are related to (C–H) alkanes with different branches.

**3.5. RP-UHPLC-MS Analysis.** Compounds along with their retention time (RT) and mass/charge ( $m/z$ ) are depicted in Tables 2 and 3 along with their names both in the positive and negative mode.

**3.6. Structure Prediction.** Protein sequence alignment revealed that regions with conserved sequences will have comparable structures and functions. After comprehensive literature, plant-based 20 phytochemicals (malonic acid, squaric acid, norvaline, allophanic acid methyl ester, 1-nitrooxypropan-2-ylazanide, DL-pyroglutamic acid, aminocap-

**Table 1. Major Peaks in IR Spectra of the Hydro-Methanolic Extract of *C. hirsuta***

| sr. no | wavenumber | functional group | sr. no | wavenumber | functional group |
|--------|------------|------------------|--------|------------|------------------|
| 1      | 684        | =C–H             | 23     | 2132       | S–C=N            |
| 2      | 752        | C–Cl             | 23     | 2398       | O=C=O            |
| 3      | 777        | C–Cl             | 24     | 2428       | O–H              |
| 4      | 823        | =C–H             | 25     | 2493       | O–H              |
| 5      | 846        | C–Cl             | 26     | 2570       | S–H              |
| 6      | 890        | C=C              | 27     | 2644       | O–H              |
| 7      | 991        | C=C              | 28     | 2730       | =C–H             |
| 8      | 1064       | –C–O             | 29     | 2857       | C–H              |
| 9      | 1094       | C–N              | 30     | 2909       | C–H              |
| 10     | 1161       | C–F              | 31     | 2948       | C–H              |
| 11     | 1278       | C–N              | 32     | 3021       | =C–H             |
| 12     | 1328       | O–H              | 33     | 3043       | C–H              |
| 13     | 1362       | –C–H             | 34     | 3132       | N–H              |
| 14     | 1399       | S=O              | 35     | 3259       | O–H              |
| 15     | 1422       | C=C              | 36     | 3347       | N–H              |
| 16     | 1436       | O–H              | 37     | 3367       | O–H              |
| 17     | 1472       | C=C              | 38     | 3490       | O–H              |
| 18     | 1507       | N–O              | 39     | 3524       | O–H              |
| 19     | 1574       | N–H              | 40     | 3548       | O–H              |
| 20     | 1595       | C=C              | 41     | 3567       | O–H              |
| 21     | 1647       | C–H              | 42     | 3630       | O–H              |
| 22     | 2040       | N=C=S            | 43     |            |                  |

**Table 2. RP-UHPLC-MS Analysis of the Hydro-Methanolic Extract of *C. hirsuta* (Negative Mode)**

| sr. no | $m/z$    | name  | RT     |
|--------|----------|---|--------|
| 1      | 103.0046 | malonic acid  | 3.335  |
| 2      | 112.9865 | squaric acid  | 2.511  |
| 3      | 243.0626 | uridine   | 4.175  |
| 4      | 293.1767 | gingerol  | 17.615 |
| 5      | 309.0487 | filiforminol  | 12.924 |
| 6      | 372.1064 | prasugrel   | 4.065  |
| 7      | 771.201  | kaempferol 3-glucoside-7-sophoroside  | 10.555 |
| 8      | 492.1053 | glucuhirsutin   | 10.579 |
| 9      | 787.1752 | quercetin 3-(6"-caffeoylsophoroside)  | 11.842 |
| 10     | 801.1738 | quercetin 3-gentiobioside-7-glucuronide   | 12.738 |
| 11     | 801.1908 | quercetin 3-(2"-feruloylsophoroside)  | 12.29  |
| 12     | 831.2013 | quercetin 3-(6"-sinapylglucosyl) (1->2)-galactoside   | 12.166 |
| 13     | 917.2387 | kaempferol 7-O-(6-trans-caffeoyl)-beta-glucopyranosyl-(1->3)-alpha-rhamnopyranoside-3-O-ketaglucopyranoside | 12.06  |
| 14     | 947.2476 | kaempferol 3,4'-diglucoside-7-(2"-ferulylglucoside)   | 12.104 |

roic acid, 3,3-dimethyl-1,2-dithiolane, vinylacetylglycine, luma-zine, 8-methylsulfinyloctyl glucosinolate, mulberrofuran-M, quercetin 3,5-digalactoside, kaempferol 3-glucoside-7-sophoro-side, quercetin 3-(6"-caffeoylsophoroside), quercetin 3-(2"-feruloylsophoroside), and kaempferol 3,4'-diglucoside-7-(2"-ferulylglucoside) were selected and searched on PubChem database. (2D) Chemical structures of chosen compounds were drawn by ChemDraw and retrieved as PDB format. Energy minimization was performed against compounds utilizing Chem3D Ultra and UCSF Chimera 1.12 (Figure 2A,B, respectively). Employing UCSF Chimera 1.12 for 1500 steps (step size 0.02), the energy minimization and structure

Table 3. RP-UHPLC-MS Analysis of the Hydro-Methanolic Extract of *C. hirsuta* (Positive Mode)

| sr. no | <i>m/z</i> | name  | RT     |
|--------|------------|---|--------|
| 15     |            | monacolin K   | 2.372  |
| 16     |            | arginine  | 2.574  |
| 17     | 116.0701   | D-proline   | 2.795  |
| 18     | 245.0757   | uridine   | 4.175  |
| 19     | 627.1567   | quercetin 3,5-digalactoside   | 10.595 |
| 20     | 220.1356   | pentahomomethionine   | 11.725 |
| 21     | 174.0942   | 2-[(isopropylthio)methyl] furan   | 11.831 |
| 22     |            | abacavir  | 11.832 |
| 23     |            | 2-hydroxyethyl-[[[3-(hydroxymethyl)-2-sulfanylideneimidazolidin-1-yl] methyl] azanium | 12.111 |
| 24     | 234.1516   | hexahomomethionine  | 12.169 |
| 25     |            | 3-amino-5-(pyridin-1-ium-1-ylmethyl) pyrazine-2-carbonitrile                          | 12.223 |
| 26     | 590.1192   | mulberrofuran M   | 12.911 |
| 27     | 803.2031   | quercetin 3-(2 <sup>'''</sup> -feruloylsophoroside)                                   | 12.292 |
| 28     | 274.2734   | sphinganine   | 15.409 |
| 29     | 286.1432   | morphine  | 18.609 |
| 30     | 279.1595   | emmotin A   | 21.753 |

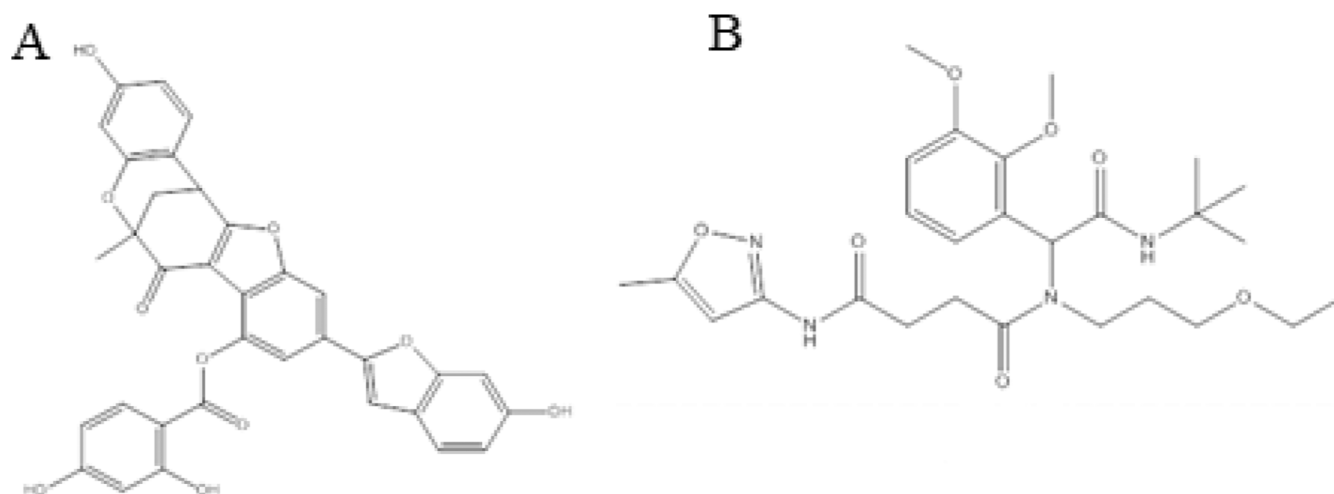


Figure 2. 2D chemical structures of top selected phytochemicals: (A) mulberrofuran M and (B) quercetin 3-(6''-caffeoylsophoroside).

optimization were carried out using the steepest and conjugate gradient methods.<sup>33</sup>

**3.7. Molecular Docking Analysis.** All phytochemicals depicted effective binding affinities against all targeted proteins as which were selected (Table 4). Highest binding affinity, lowest binding energy, and ADMET characteristics were used to categorize docked complexes, and the top two compounds [mulberrofuran-M and quercetin3-(6''caffeoylsophoroside)] were chosen for each protein during docking analyses. The molecular interactions of these docked complexes were examined critically. The conformational binding pattern of the phytochemicals, showed their similar binding position in the active pocket of receptor proteins. Docking studies of the mulberrofuran-M exhibited its binding at the active site of TNF- $\alpha$  (Gln-17, Leu-18, Glu-19, Leu-35, Asp-37, Asn-38, Lys-81, Glu-126, Val-127, and Pro-130). Results were depicted in (Figure 3A). The phytochemical showed good binding affinities (-8.2 Kcal/mol) against targeted protein as compared to other compounds. In the docking studies of quercetin 3-(6''-caffeoylsophoroside) with GSK-3 $\beta$ , the post docking analyses was critically observed on the basis of their binding energies (Glu-80, Asp-105, His-106, Cys-107, Arg-111, Arg-113, Asp-133, Tyr-134, Val-135, Pro-136, Asp-190, Val-195, Thr-193, Lys-197, Pro-357, Ala-358, and Asn-361).

Table 4. Binding Affinities (Kcal/mol) Calculations of Compounds against Diabetes Targeted

| chemical compounds                                    | TNF- $\alpha$ | AKT-1 | GSK-3 $\beta$ |
|---|---------------|-------|---------------|
| malonic acid  | -4.8          | -5.0  | -3.6          |
| squaric acid  | -4.5          | -6.6  | -5.2          |
| norvaline   | -3.4          | -5.4  | -3.9          |
| allophanic acid methyl ester                          | -3.7          | -4.8  | -4.0          |
| 1-nitrooxypropan-2-ylazaniide                         | -3.7          | -4.5  | -3.7          |
| DL-pyroglyutamic acid                                 | -4.5          | -5.3  | -4.3          |
| aminocaproic acid                                     | -3.9          | -4.8  | -4.1          |
| 3,3-dimethyl-1,2-dithiolane                           | -2.8          | -4.3  | -3.5          |
| vinylacetylglucine                                    | -4.0          |       | -4.4          |
| lumazine  | -4.8          | -6.3  | -5.4          |
| 8-methylsulfinyloctyl glucosinolate                   | -5.8          | -7.1  | -5.7          |
| 3,4-dihydroxybenzoic acid                             | -5.0          | -6.7  | -5.2          |
| mulberrofuran M                                       | -8.2          | -6.6  | -7.4          |
| quercetin 3,5-digalactoside                           | -7.0          | -5.2  | -6.7          |
| kaempferol 3-glucoside-7-sophoroside                  | -7.4          | -2.5  | -3.3          |
| quercetin 3-(6''-caffeoylsophoroside)                 | -7.2          | -7.2  | -7.2          |
| quercetin 3-(2 <sup>'''</sup> -feruloylsophoroside)   | -7.1          | -0.8  | -5.8          |
| kaempferol 3,4'-diglucoside-7-(2''-feruloylglucoside) | -6.8          | -4.0  | -3.6          |

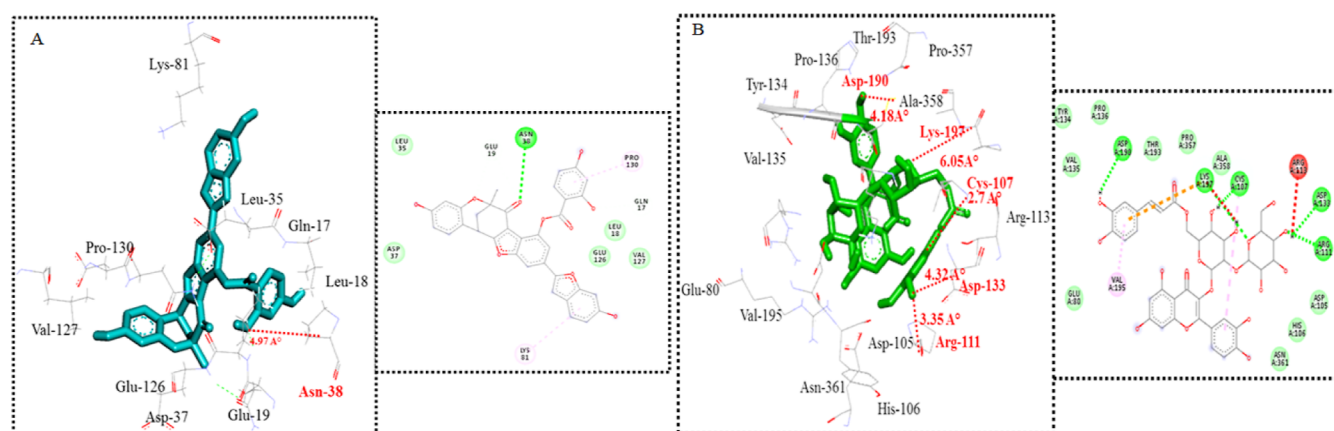


**Figure 3.** Molecular docking. 2D and 3D molecular interactions of top docked complex of 1st top compound mulberrofuran M ( $-8.2$  Kcal/mol) against targeted receptor of TNF- $\alpha$  (A). 2D and 3D molecular interactions of top docked complex of 3rd top compound quercetin 3-(6''-caffeoylsophoroside) ( $-7.2$  Kcal/mol) against targeted receptor of GSK-3 $\beta$  (B).

Results were depicted in (Figure 3B). The lowest binding affinity of ( $-7.2$  Kcal/mol) was observed and key interactive residues were also observed. Molecular docking analyses of the chosen inhibitors revealed variations in the observed binding energies, and among all the created docking complexes for each inhibitor, the appropriate docked complex with the lowest binding energy was chosen. By using the internet programme mClue, drug-like properties were observed (Table 4). The ADMET properties, toxicity, and carcinogenicity were also calculated for the top selected inhibitors (Table 5). The inhibitors having the cyclic rings showed important biological characteristics.

**Table 5. ADMET Properties of Top Two Selected Phytocompounds**

| properties                  | mulberrofuran M                     | quercetin 3-(6''-caffeoylsophoroside) |
|-----------------------------|-------------------------------------|---------------------------------------|
| Blood–Brain Barrier         | BBB+<br>0.5492                      | BBB–<br>(0.7002)                      |
| Human Intestinal absorption | HIA+<br>0.9651                      | HIA+<br>(0.7179)                      |
| AMES toxicity               | non- AMES toxic<br>0.8716           | AMES toxic<br>0.7010                  |
| carcinogens                 | non-carcinogens<br>0.9281           | non-carcinogens<br>0.9526             |
| biodegradation              | not readily biodegradable<br>0.9837 | not readily biodegradable<br>0.8433   |
| acute oral toxicity         | III<br>0.5666                       | IV<br>0.4410                          |
| aqueous solubility (Logs)   | $-3.6970$                           | $-2.6290$                             |

**3.8. Acute Oral Toxicity.** Acute toxicity testing revealed no mortality, proving that the *C. hirsuta* hydro-methanolic extract is safe for use in anti-diabetic research.

**3.9. Water Intake.** An increase in water intake (mL/day/100 g BW) was observed in the hydro-methanolic extract of *C. hirsuta* treated groups in a dose-dependent fashion comparative to the HFD-STZ disease group, as shown in Table 6.

**3.10. In Vivo Anti-Diabetic Activity.** Figure 4A shows the fasting blood glucose levels. After STZ injection, the group HFD-STZ glucose levels increased dramatically ( $>400$  mg/dL)

compared to group NC (100 mg/dL) and remained at this high level until the end of the experiment. In contrast, the glucose level in groups HFD-STD and HFD-STZ 125–500 mg/kg was significantly lowered than that in group HFD-STZ following STZ injection. FBG levels ( $468 \pm 27.2$ ) mg/dL drastically increased in the HFD-STZ diabetic group, while reverted ( $74.2 \pm 3.27$ ) mg/dL in a dose-dependent fashion in HFD-STZ-treated groups. FINS levels ( $6.55 \pm 0.221$ )  $\mu$ U/mL decreased in the HFD-STZ group but it was improved in the HFD-STZ 500 treated group ( $13.2 \pm 0.665$ )  $\mu$ U/mL, shown in Figure 4B. The rats were also observed for their improvement in glycosylated hemoglobin (HbA1c) on treatment with the hydro-methanolic extract of *C. hirsuta*. Significant improvement (Figure 4C) in the HFD-STZ 500 group ( $10 \pm 0.20$  mg/dL) was observed as compared to the HFD-STZ group ( $16.36 \pm 0.18$  mg/dL) after treatment with the hydro-methanolic extract of *C. hirsuta*.

**3.11. Biochemical Analysis.** Impact of various doses (500, 250, and 125 mg/kg) of *C. hirsuta* hydro-methanolic extract on the levels of serum lipids in diabetic rats was checked. Serum levels of the diabetic control group were considerably higher ( $p < 0.001$ ) than those of the normal control and the *C. hirsuta*-treated groups (Table 7). Increased serum levels returned to normal after treatment with *C. hirsuta* hydro-methanolic extract. However, HDL levels in the disease control group were significantly lower than other groups.

The liver function tests ALT, AST, and ALP of blood samples collected from rats at the 60th day of study revealed the significant improvement in the plasma samples of hydro-methanolic extract of *C. hirsuta*-treated rats. The increased values of enzymes due to induction with streptozotocin were restored close to normal Figure 5A–C by administration of the hydro-methanolic extract of *C. hirsuta* (HFD-STZ 125–500 mg/kg). The hydro-methanolic extract of *C. hirsuta* lowered, elevated levels of serum urea and creatinine in diabetic rats Figure 5D,E.

Liver and skeletal muscle glycogen levels were reduced in diabetic rats ( $p < 0.001$ ) (Table 8). Treatment with the hydro-methanolic extract of *C. hirsuta* restored the concentrations of glycogen both in liver and skeletal muscles.

**3.12. Relative Weight of Organs (Liver, Pancreas, and Kidney).** Internal organs were collected for relative weight study. Decreased weight of liver ( $7.82 \pm 0.21$ ) g, pancreas ( $0.48 \pm 0.025$ ) g, and kidney ( $0.56 \pm 0.077$ ) g were observed

Table 6. Effect of Water Intake in Hydro-Methanolic Extract of *C. hirsute*-Treated HFD-SD Rats

| Sprague-Dawley rats Groups | water intake (mL/day/100 g BW) |                    |                 |
|----------------------------|--------------------------------|--------------------|-----------------|
|                            | day 0                          | dAY 30             | day 60          |
| normal control (NC)        | 5.81 ± 1.68                    | 6.24 ± 1.7         | 9.75 ± 1.93     |
| HFD-STZ (diabetic control) | 11.3 ± 1.92***                 | 13.5 ± 2.26***     | 22.9 ± 4.31***  |
| HFD-STD (positive control) | 6.5 ± 0.75S###                 | 8.42 ± 0.44###     | 21.6 ± 0.922*** |
| HFD-STZ 500 mg/kg          | 7.04 ± 0.702##                 | 10.8 ± 0.828***#   | 21.8 ± 0.941*** |
| HFD-STZ 250 mg/kg          | 10.4 ± 1.51***                 | 12.7 ± 0.672*** ns | 21.5 ± 2.14***  |
| HFD-STZ 125 mg/kg          | 7.69 ± 1.24##                  | 8.98 ± 0.598*###   | 22 ± 0.782***   |

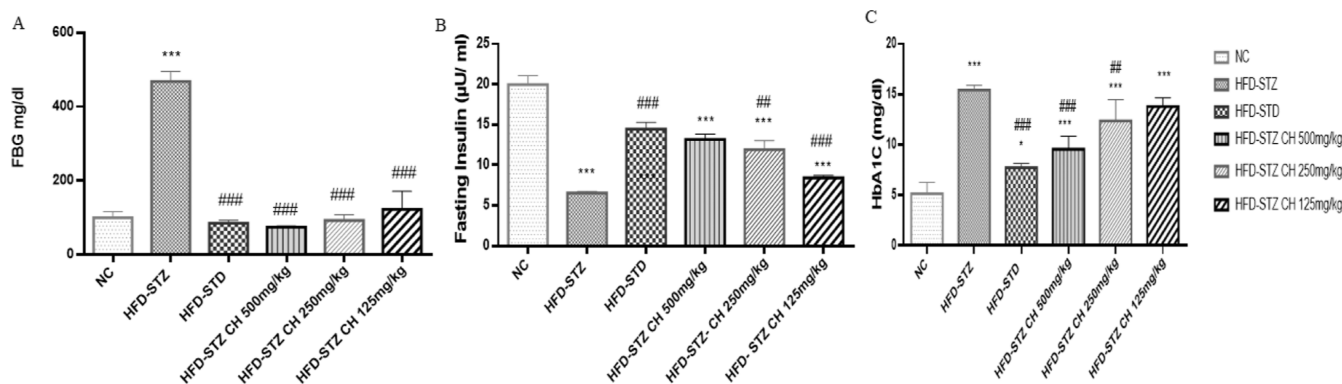


Figure 4. Effect of hydro-methanolic extract of *C. hirsute* on (A). Fasting blood glucose FBG (mg/dL) level. (B) Fasting insulin levels ( $\mu\text{U}/\text{mL}$ ), (C) HbA1C levels (mg/dL). Data are presented as mean  $\pm$  SD,  $n = 3$ . Where  $P^* < 0.05$ ,  $P^{**} < 0.01$ , and  $P^{***} < 0.001$ .

Table 7. Effect of the Hydro-Methanolic Extract of *C. hirsute* on Analysis of the Lipid Profile

| Sprague-Dawley rat Groups  | total cholesterol (mg/dL) | triglycerides (mg/dL)  | HDL (mg/dL)                       | LDL (mg/dL)            | VLDL (mg/dL)           |
|----------------------------|---------------------------|------------------------|-----------------------------------|------------------------|------------------------|
| normal control (NC)        | 75.3 $\pm$ 3.95           | 32.6 $\pm$ 7.35        | 41 $\pm$ 2.11                     | 20 $\pm$ 4.65          | 27.3 $\pm$ 0.561       |
| HFD-STZ (diabetic control) | 187 $\pm$ 1.13***         | 168 $\pm$ 6.88***      | 25.4 $\pm$ 1.23***                | 112 $\pm$ 13.8***      | 34.4 $\pm$ 0.939***    |
| HFD-STD (positive control) | 81.8 $\pm$ 1.27*###       | 42.3 $\pm$ 1.67*       | 38.8 $\pm$ 1.02 <sup>ns</sup> ### | 37.9 $\pm$ 0.464*##### | 24.2 $\pm$ 0.543*##### |
| HFD-STZ 500 mg/kg          | 109 $\pm$ 4.88***###      | 44.7 $\pm$ 0.924*##### | 36.5 $\pm$ 0.91***###             | 39.8 $\pm$ 0.839*##### | 26.2 $\pm$ 0.415###    |
| HFD-STZ 250 mg/kg          | 116 $\pm$ 1.29***###      | 46.5 $\pm$ 0.68***###  | 32.8 $\pm$ 0.615*#####            | 46.6 $\pm$ 1.7*#####   | 30 $\pm$ 0.716*#####   |
| HFD-STZ 125 mg/kg          | 119 $\pm$ 1.03***###      | 47.6 $\pm$ 0.899*##### | 29.1 $\pm$ 1.22***###             | 49.7 $\pm$ 0.941*##### | 32.6 $\pm$ 0.573*##### |

in a diabetic group, but improvement was observed in extract-treated groups; the weight of liver ( $11.8 \pm 0.312$ ) g, pancreas ( $0.692 \pm 0.0421$ ) g, and kidney ( $0.99 \pm 0.0374$ ) g were improved and presented in Table 9.

**3.13. Urine Analysis.** The urine of the rats was also collected after 12 h of fasting. Urinalysis revealed the presence of glucose, ketone bodies, and appearance of dark yellow urine. Urine volume increased in the diabetic group which upon treatment with HFD-STZ 125–500 mg/kg decreased in treatment groups exhibiting a dose-dependent pattern. Additionally, the extract treatment also decreased the levels of urinary parameters; creatinine ( $67.6 \pm 2.03$ ) and urea ( $2.13 \pm 0.0876$ ) as compared to the diabetic group ( $16.4 \pm 1.37$ ) and ( $0.648 \pm 0.054$ ), respectively (Figure 6A–D).

**3.14. Oxidative Stress Biomarkers.** The hydro-methanolic extract of *C. hirsute*, possesses antioxidant properties, which scavenged the oxidative stress caused by STZ. This effect was seen at different doses in serum, whole blood (hemolysate), liver, pancreatic, and kidney tissues samples of HFD SD rats (Table 10). The present study indicated the elevation of MDA contents, a reliable marker of lipid peroxidation in the serum, pancreatic, renal, and hepatic tissue homogenate after STZ induction with a significant ( $p < 0.001$ ) in the HFD-STZ disease group, while treatment with the hydro-methanolic extract of *C. hirsute* (HFD-STZ 500, 250, and 125 mg/kg) significantly ( $p < 0.001$ ) reduced the MDA

level to normalcy. T.AOC, GSH-ST, GS-PX, and CAT activities were considerably ( $p < 0.001$ ) decreased in pancreas, kidney, liver, and serum/blood samples of STZ-induced diabetic rats. Significant restoration was achieved by oral intubation of *C. hirsute* hydro-methanolic extract (HFD-STZ 500, 250, and 125 mg/kg). Similarly, serum G6PD levels returned to normal after being treated with the *C. hirsute* hydro-methanolic extract in positive control HFD-STD and dose groups (HFD-STZ 500, 250, and 125 mg/kg).

**3.15. Histopathological Examination.** The liver, kidney, and pancreatic tissues in the control group were found to be in normal condition without any pathological alterations. The loss of islet cells, swollen acinar cells in the pancreatic tissues, and the deterioration of hepatocytes, as well as vacuolization of the cytoplasm and hazy swelling, were all symptoms of significant pathological damage in the diabetic rat tissues induced by STZ (55 mg/kg). Animal tissues treated with glibenclamide (600 g/kg) and extract showed significant improvements in degenerative alterations in renal tubules and pancreatic acinar cells, congestion in the central vein, and loss of glycogen granules (Figure 7).

## 4. DISCUSSION

Type 2 DM is usually characterized by elevated plasma glucose levels along with increased cholesterol levels.<sup>34</sup> Since

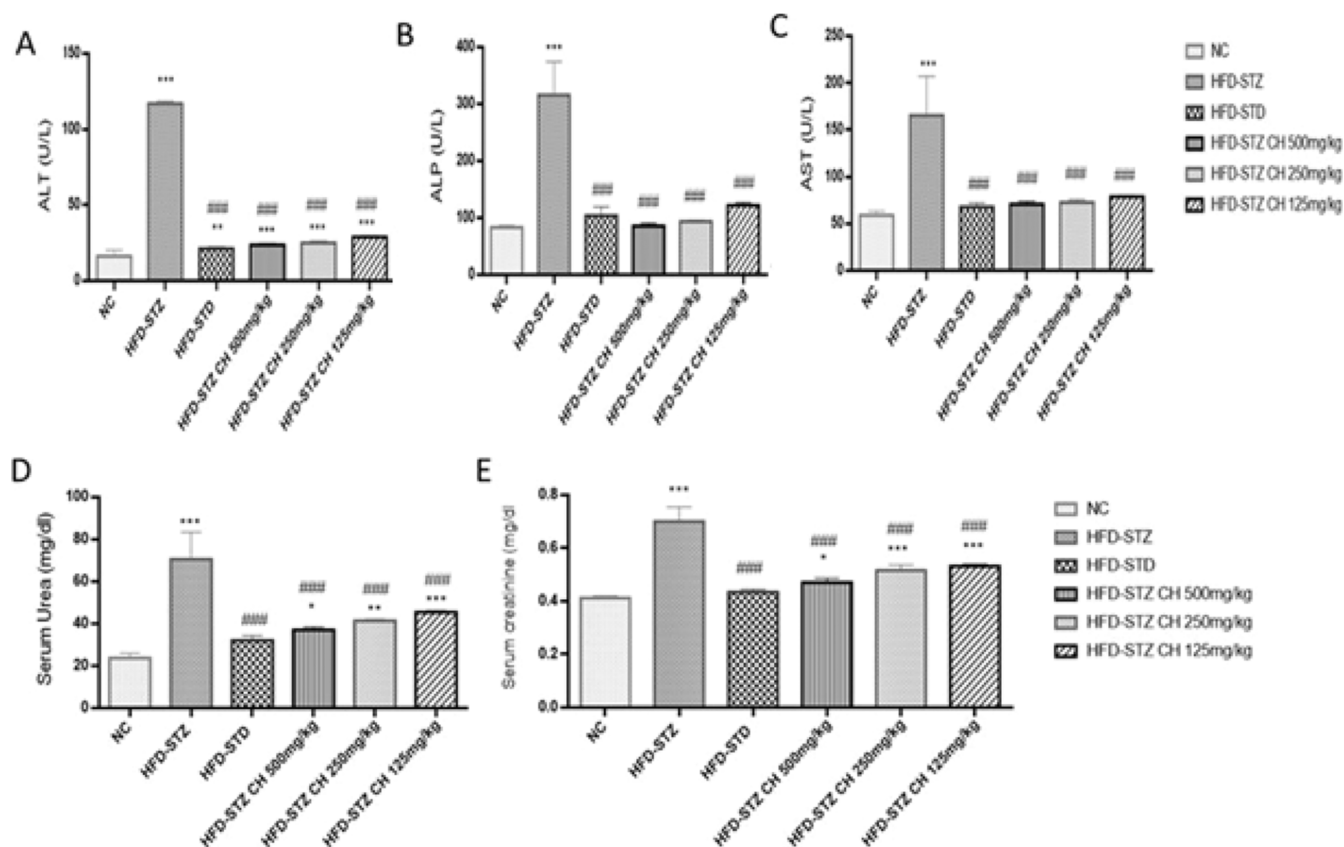


**Figure 5.** Effects of hydro-methanolic extract of *C. hirsuta*. (A) Alanine amino transferase (ALT) U/L. (B) Alkaline phosphatase (ALP) U/L. (C) Aspartate aminotransferase (AST) U/L. (D) Serum urea (mg/dL) levels. (E) Serum creatinine (mg/dL) levels. Data are presented as mean  $\pm$  SD,  $n = 3$ . Where  $P^* < 0.05$ ,  $P^{**} < 0.01$ , and  $P^{***} < 0.001$ .

**Table 8.** Effect of Hydro-Methanolic Extract of *C. hirsuta* Liver and Skeletal Muscle Glycogen Levels

|                                      | NC               | HFD-STZ                | HFD-STD            | HFD-500 mg/kg           | HFD-250 mg/kg       | HFD-125 mg/kg          |
|--------------------------------------|------------------|------------------------|--------------------|-------------------------|---------------------|------------------------|
| liver glycogen (mg/g liver tissue)   | 16.9 $\pm$ 0.416 | 7.36 $\pm$ 0.234***### | 13.4 $\pm$ 2.54**  | 11.3 $\pm$ 2.16***      | 10.3 $\pm$ 0.389*** | 9.35 $\pm$ 0.2***      |
| muscle glycogen (mg/g muscle tissue) | 1.2 $\pm$ 0.288  | 0.1 $\pm$ 0.0675***### | 0.979 $\pm$ 0.0234 | 0.348 $\pm$ 0.112***### | 0.859 $\pm$ 0.13*   | 0.445 $\pm$ 0.17***### |

prehistoric days, conventional remedies for the treatment of type 2 DM have included the use of plants with therapeutic characteristics.<sup>35</sup> The effect of the hydro-methanolic extract of *C. hirsuta* on HFD-STZ-induced diabetic rats was checked during the acute toxicity study which indicated that up to 2000 mg/kg dose is safe in SD rats selected for experiment. Occurrence of many phenolics and flavonoids in the extract were confirmed by RP-UHPLC coupled to DAD and RP-UHPLC-MS.<sup>36</sup> Several biomolecules such as malonic acid,<sup>37</sup> squaric acid,<sup>38</sup> D-proline,<sup>39</sup> and uridine<sup>40</sup> were quantified in the hydro-methanolic extract of *C. hirsuta*. Polyphenols were also detected in plant extracts during previous studies. It was speculated that polyphenols reduce the risk of degenerative diseases by acting as an antioxidant defense against the stress developed due to oxidation.<sup>41</sup> Higher number of phenolic compounds in plant extract might be linked with more antioxidant capacity. The compounds identified by RP-UHPLC-MS were widely reported as potent antioxidants such as kaempferol 3-glucoside-7-sophoroside,<sup>42</sup> arginine,<sup>43</sup> sphinganine,<sup>44</sup> emmotin A,<sup>45</sup> and lumazine.<sup>46</sup> These compounds have the ability to halt oxidation chain reaction due to their reducing properties, This will aid in absorption and

neutralization of scavenging radicals, the quenching of singlet and triplet oxygen, or the breakdown of peroxides. Results of the current study are supported by in vitro and in vivo assays which examined the antioxidant potential of different extracts of *C. hirsuta*.<sup>47</sup> FTIR analysis was performed on the plant extract to identify any potential bonding with bends and stretching of different chemical groups in the extract which was confirmed due to presence of characteristic peaks of phenols, alkaloids, sulfur-containing compounds, olefins, alkanes, alcohols, and alkyl halides. The presence of such groups with bends and stretches in FTIR data of plant extracts was also evident from previous studies.<sup>48</sup> Polyphenols such as monacolin K, pectolarin, and gingerol with antidiabetic activity have the potential to block glucoside hydrolases due to their capacity to link with proteins. Moreover, these compounds can boost antioxidant defenses, increase glucokinase activity, and reduce lipid peroxidation along with the increase in insulin release. Monacolin K can increase pancreatic insulin expression and lessen pancreatic dysfunction created by advanced glycation end products.<sup>49</sup> A flavone pectolarin can improve severely dysregulated diponectin expression in HFD-STZ diabetic rats and can upgrade glucose homeostasis.<sup>50</sup>



Table 9. Effect of Hydro-Methanolic Extract of *C. hirsuta* on Relative Weight of Organs (Liver, Pancreas, and Kidney) of Rats

| Sprague-Dawley rat Groups  | weight of pancreas  | weight of liver   | weight of kidney  | relative weight of pancreas | relative weight of kidney | relative weight of liver |
|----------------------------|---------------------|-------------------|-------------------|-----------------------------|---------------------------|--------------------------|
| normal control (NC)        | 1.32 ± 0.262        | 12.6 ± 0.303      | 1.06 ± 0.027      | 0.698 ± 0.0994              | 0.57 ± 0.0991             | 6.3237 ± 1.1224          |
| HFD-STZ (diabetic control) | 0.48 ± 0.0255***    | 7.82 ± 0.21***    | 0.56 ± 0.0778***  | 0.488 ± 0.0206*****         | 0.644 ± 0.0536            | 7.7848 ± 0.20155**       |
| HFD-STD (positive control) | 0.894 ± 0.0695***** | 12.3 ± 0.307###   | 1.04 ± 0.225###   | 0.323 ± 0.0309*****         | 0.374 ± 0.0844*****       | 4.5587 ± 0.22334*****    |
| HFD-STZ 500 mg/kg          | 0.692 ± 0.0421***   | 11.8 ± 0.312***   | 0.99 ± 0.0374###  | 0.277 ± 0.0132*****         | 0.408 ± 0.0288*****       | 5.1945 ± 0.13243***      |
| HFD-STZ 250 mg/kg          | 0.644 ± 0.0365***** | 11.6 ± 0.426***   | 0.882 ± 0.0277### | 0.288 ± 0.0159*****         | 0.394 ± 0.00916*****      | 5.1925 ± 0.18716***      |
| HFD-STZ 125 mg/kg          | 0.594 ± 0.0114***** | 11.2 ± 0.674***** | 0.808 ± 0.0676**  | 0.283 ± 0.0112*****         | 0.385 ± 0.035*****        | 5.3656 ± 0.26636###      |

Gingerol is also an effective hypoglycemic with improved insulin sensitivity and reduced hyperlipidemia in type 2 DM.<sup>51</sup>

According to Phoebe Chen and Chen, (2008).<sup>52</sup> Bioinformatics is a cutting-edge, quick method of drug creation with significant outcomes.<sup>53</sup> The goal of the current study was to determine the effectiveness of plant-derived phytochemicals [mulberrofuran-M and quercetin 3-(6''-caffeoylso-phoroside)] against three target proteins: TNF- $\alpha$ , GSK-3, and AKT-1 in type 2 DM.

Post docking analyses of mulberrofuran-M with TNF- $\alpha$  exhibited a single H-bonding interaction at Asn-38 having bond distances 4.97 Å. Similarly, in quercetin 3-(6''-caffeoylso-phoroside) against GSK-3 $\beta$  docking complex, number of (H) bonding interactions were observed as compared to other docked complexes. There are five hydrogen bonding interactions at different interactive residues. Arg-111, Cys-107, Asp-133, Asp-190, and Lys-197, with 3.35, 2.07, 4.32, 4.18, and 6.05 Å bond lengths. In this study, the compounds have exhibited significant anti-diabetic activity evident from drug likeness and ADMET profile. The blood–brain barrier (BBB) index is extremely important for drug transport and is considered an efficient barrier for filtration of constituents which are harmful for performance of brain.<sup>54</sup> Intestinal absorption in humans depends on the physicochemical properties of compounds, so it is a vital factor in drug activity.

Both mulberrofuran M and quercetin 3-(6''-caffeoylso-phoro-side) have a better ADMET profile. However, quercetin 3-(6''-caffeoylso-phoroside) has better ability to cross the BBB.

Biodegradation is important characteristic of phytochemicals. Fading of phytochemicals in environment termed as biotransformation which may be toxic to terrestrial and aquatic ecosystems. If they are not easily or effectively degraded, these may produce CO<sub>2</sub> and a number of reactive intermediates.<sup>54,55</sup>

In silico ADMET profile analysis is a beneficial technique to check compound's pharmacokinetic characteristics as it can detect factors related to compound like biodegradability, bioavailability, blood–brain barrier, pharmacological toxicity, and carcinogenicity quickly. In silico ADMET profile analysis suggest that both compounds mulberrofuran M and quercetin 3-(6''-caffeoylso-phoroside) are not ready for biodegradation but mulberrofuran M was neither carcinogenic nor AMES hazardous, with the exception of quercetin 3-(6''-caffeoylso-phoroside), which is solely AMES harmful. These substances are strong candidates for use as antidiabetic medicines according to molecular docking studies of the active compounds and drug similarity features.

Elevated levels of serum urea and creatinine is hallmark of hypoglycemia.<sup>56</sup> Renal insufficiency greatly linked with type 2 DM, hypertension, and hypertriglyceridemia. The hydro-methanolic extract of *C. hirsuta* considerably reduces serum urea and creatinine levels in HFD-STZ diabetic rats; however, the exact mechanism for above still has to be investigated. During hyperlipidemia elevated levels of free fatty acids in serum of diabetic rats can prevent entry of glucose into cells by accumulation on the arterial walls and transportation of fatty plaques into the liver via HDL. This demonstrates the therapeutic benefits of higher HDL and lower cholesterol and triglyceride levels. The results of the current study showed that HFD STZ diabetic rats had an increase in lipidemia, as seen by elevated TG, LDL, and in HFD STZ diabetic rats. These reduced indices were most likely caused by the presence of quercetin and kaempferol analogues, which decreased the hepatic lipid profiles and exhibited hypolipidemia. The increase

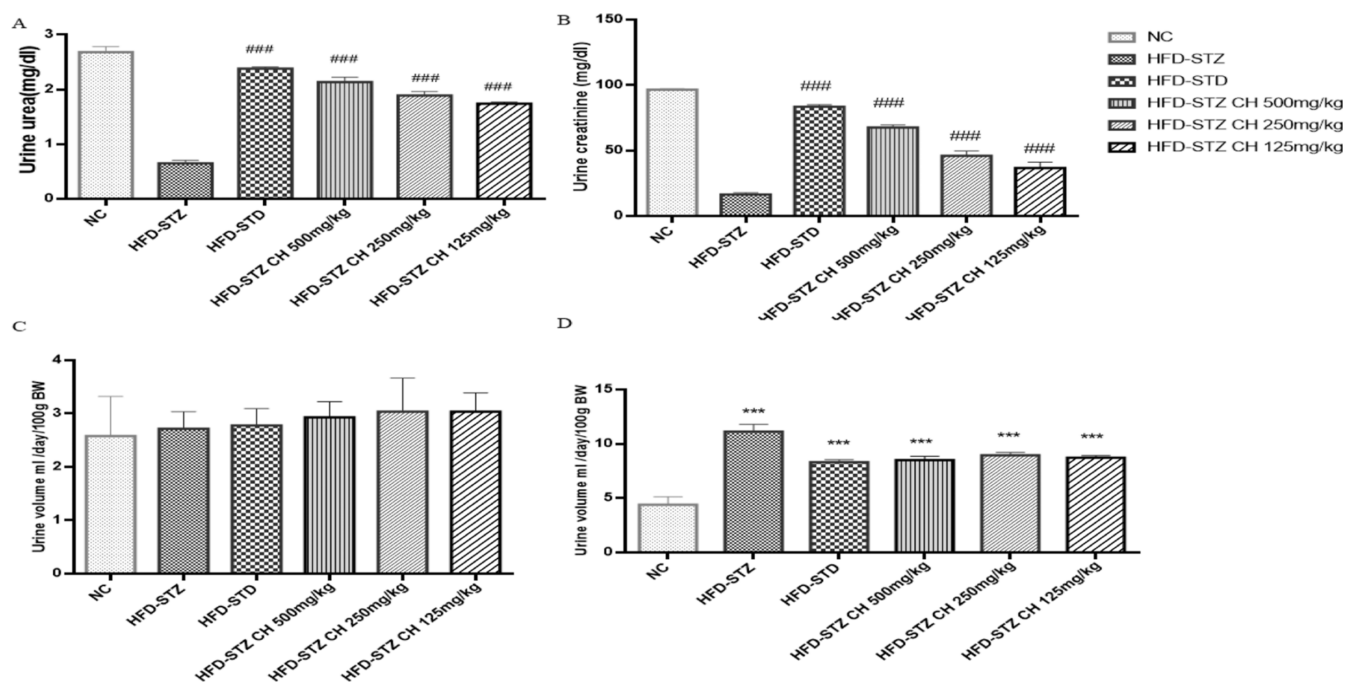


**Figure 6.** Effect of the hydro-methanolic extract of *C. hirsuta* on (A) urinary urea (mg/dL) levels, (B) urinary creatinine (mg/dL) levels, (C) urinary output at day 0, and (D) urinary output at last day (mL/day/100 g BW). Data are presented as mean  $\pm$  SD,  $n = 3$ . Where  $P^* < 0.05$ ,  $P^{**} < 0.01$ , and  $P^{***} < 0.001$ .

in glycated hemoglobin HbA1c in diabetic rats is associated with higher glycation of hemoglobin under hyperglycemia upon administration of HFD-STZ. It was also reduced in the HFD-STZ treatment groups due to inhibition of the reaction of more glucose present in the blood with hemoglobin to form HbA1C, which might be due to presence of antioxidants phytoconstituents that possess protein glycation inhibitory effects associated with type 2 DM.<sup>57</sup> Phyto-constituents in the hydro-methanolic extract of *C. hirsuta* possess the free radical scavenging potential which is responsible for the improvement in the liver markers ALT, AST, and ALP. Decline of enhanced liver markers might be due to reduction in free fatty acids (FFAs), peroxides in the serum, and decreased oxidation linked with amelioration of hepatic transaminases and phosphatase.<sup>58</sup>

Alterations in the weight of kidney can be linked to an increased rate of protein synthesis and a decreased degradation of renal ECM components as an immediate response to diabetic induction. Despite liver enlargement, the increased relative weight of the liver is a direct result of triglyceride buildup, free fatty acid efflux due to hyperinsulinemia, and the poor liver-excreted lipoprotein production resulting in apolipoprotein B insufficiency. Whereas in diabetic rats, the loss of pancreatic islets and the selective apoptosis of insulin-producing cells caused a drop in pancreatic weight proportional to body weight.<sup>59</sup> STZ induction triggered hyperglycemia which suppresses the generation of insulin and causes glucose to enter the beta cells of the pancreas through the glucose transporter 2 (GLUT2). The slow absorption of the plant extract may have contributed to the extraordinary glucose-lowering impact seen in the current study. Lower FBG levels in HFD-STZ treated rats might be due to presence of quercetin, which has the capacity to trigger the release of insulin.<sup>60</sup>

An imbalance between the body's antioxidant defenses and reactive oxygen products leads to oxidative stress which effects pathologies of type 2 DM and has an ability to deteriorate diabetic complications and production of ROS.<sup>61</sup> The reduction in insulin release from  $\beta$  cells and the increase in insulin resistance are both driven by this surge in oxidative stress. Diffusion of ROS inside of cells results in DNA and mitochondrial damage.<sup>62</sup> The presence of SOD and CAT enzymes in all oxygen metabolizing cells help in averting damage to cells by free radicals with the provision of a repair mechanism. The extract of *C. hirsuta* exhibited both in vitro and in vivo potent antioxidant potential. MDA levels which are lipid peroxidation end products are decreased in HFD-STZ-treated groups due to treatment with the extract, whereas GST levels and GS-PX activity are increased.<sup>62</sup>

Due to increased water intake and urine volume, glucosuria was seen in diabetic rats. Urea and creatinine levels were lower in the urine while increasing in the serum due to excess production after increased protein metabolism. The hydro-methanolic extract of *C. hirsuta* dramatically improved urinary urea and creatinine levels.<sup>63</sup> Urinary urea and creatinine levels restored significantly upon treatment with the hydro-methanolic extract of *C. hirsuta*.

## 5. CONCLUSIONS

The current study's results indicated that *C. hirsuta* hydro-methanolic extract considerably aided in glucose reduction, stabilized glycated hemoglobin (HbA1C), inhibited  $\alpha$ -amylase, and improved the status of lipid profiles. *C. hirsuta* hydro-methanolic extract may have protective effects against hyperglycemia by reducing the rise in oxidative stress and inflammation in type 2 DM in HFD-STZ SD rats. Therefore, the current study proposes that following carefully monitored clinical trials, the hydro-methanolic extract of *C. hirsuta* may be

Table 10. Effect of the Hydro-Methanolic Extract of *C. hirsuta* on Oxidative Stress Marker

| MDA content (nmol/mg prot.)     | NC            | HFD-STZ             | HFD-STD          | HFD-500 mg/kg      | HFD-250 mg/kg       | HFD-125 mg/kg       |
|---------------------------------|---------------|---------------------|------------------|--------------------|---------------------|---------------------|
| pancreas                        | 2.21 ± 0.0114 | 3.99 ± 0.0321*****  | 2.32 ± 0.0249**  | 2.48 ± 0.0693***** | 2.48 ± 0.0195*****  | 2.43 ± 0.0228*****  |
| liver                           | 3.33 ± 0.0404 | 5.56 ± 0.329*****   | 3.58 ± 0.0958    | 3.65 ± 0.0396*     | 3.77 ± 0.0801**     | 3.78 ± 0.0779**     |
| kidney                          | 1.44 ± 0.023  | 3.76 ± 0.0212*****  | 1.53 ± 0.027     | 1.96 ± 0.023*****  | 2.71 ± 0.178*****   | 2.44 ± 0.48***      |
| blood serum (nmol/mL)           | 2.33 ± 0.0445 | 5.65 ± 0.193*****   | 2.84 ± 0.167***  | 3.03 ± 0.151*****  | 4.21 ± 0.198*****   | 4.02 ± 0.0487*****  |
| SOD Activity (U/mg Protein)     |               |                     |                  |                    |                     |                     |
| pancreas                        | 337 ± 25.3    | 79.7 ± 39*****      | 241 ± 25.2***    | 204 ± 7.24***      | 164 ± 5.92*****     | 135 ± 14.4*****     |
| liver                           | 369 ± 34.7    | 152 ± 26.3*****     | 329 ± 29.6       | 314 ± 52.7         | 247 ± 14.3*****     | 210 ± 35.3*****     |
| kidney                          | 289 ± 7.5     | 71.8 ± 9.45*****    | 230 ± 14.3***    | 211 ± 21.4***      | 91.9 ± 4.17*****    | 84.5 ± 4.47*****    |
| blood serum (U/mL)              | 313 ± 39.4    | 138 ± 4.66*****     | 293 ± 10.1       | 285 ± 9.98         | 244 ± 16.3*****     | 161 ± 27.6*****     |
| T.AOC Activity (U/mg)           |               |                     |                  |                    |                     |                     |
| pancreas                        | 2.81 ± 0.0339 | 1.138 ± 0.2329***** | 2.526 ± 0.05413* | 2.48 ± 0.04848*    | 2.194 ± 0.1658***** | 1.344 ± 0.1841***** |
| liver                           | 3.48 ± 0.121  | 1.32 ± 0.191*****   | 2.37 ± 0.157***  | 2.55 ± 0.0626***   | 2.16 ± 0.0396***    | 1.92 ± 0.14*****    |
| kidney                          | 2.47 ± 0.103  | 0.458 ± 0.0223***** | 1.91 ± 0.181**   | 1.54 ± 0.0293***   | 1.02 ± 0.408*****   | 1.2 ± 0.232*****    |
| blood serum (nmol/mL)           | 78.6 ± 6.86   | 23.8 ± 1.3*****     | 85.8 ± 10.3      | 56.3 ± 0.652*****  | 55.4 ± 2.9*****     | 46.5 ± 0.939*****   |
| GSH-ST Activity (U/mg Protein)  |               |                     |                  |                    |                     |                     |
| pancreas                        | 8.47 ± 0.247  | 4.15 ± 0.0399*****  | 6.34 ± 0.265     | 5.76 ± 0.299*****  | 5.36 ± 0.239*****   | 5 ± 0.112*****      |
| liver                           | 18.2 ± 0.223  | 4.14 ± 0.0929*****  | 16.8 ± 0.378***  | 15.4 ± 0.324*****  | 15.1 ± 0.0973*****  | 13.2 ± 0.894*****   |
| kidney                          | 8.8 ± 0.332   | 4.16 ± 0.111*****   | 6.86 ± 0.187***  | 5.81 ± 0.294*****  | 5.41 ± 0.259*****   | 5.2 ± 0.158*****    |
| blood serum (U/mL)              | 9.1 ± 1.62    | 3.7 ± 0.474*****    | 8.7 ± 0.673      | 5.82 ± 0.622*****  | 5.27 ± 0.0565*****  | 5.06 ± 0.0932*****  |
| GS-PX Activity (U)              |               |                     |                  |                    |                     |                     |
| pancreas                        | 1131 ± 92.13  | 865 ± 37.42*****    | 1113 ± 2.074     | 1092 ± 1.074       | 1061 ± 21.95        | 1079 ± 44.58        |
| liver                           | 560 ± 1.11    | 380 ± 40.3*****     | 556 ± 6.59       | 534 ± 23.3         | 504 ± 36***         | 459 ± 18.1*****     |
| kidney                          | 47.1 ± 1.39   | 24.7 ± 3.85*****    | 45.6 ± 0.965     | 43.1 ± 1.46        | 42.7 ± 0.694*       | 35.6 ± 2.21*****    |
| blood serum                     | 688 ± 164.4   | 355.7 ± 40.12**     | 580.4 ± 160.4    | 634.1 ± 161.8      | 626.6 ± 152.9       | 622.2 ± 36.7        |
| Catalase Activity (U/g Protein) |               |                     |                  |                    |                     |                     |
| pancreas                        | 21.6 ± 1.06   | 12.7 ± 2.21***      | 19.9 ± 0.665     | 18.4 ± 0.39**      | 17.3 ± 0.76***      | 16.2 ± 0.757*****   |
| liver                           | 477 ± 19      | 266 ± 34.1###       | 467 ± 21.6***    | 456 ± 23.6         | 414 ± 11.7###       | 398 ± 5.74*****     |
| kidney                          | 58.9 ± 1.25   | 23.8 ± 1.4*****     | 56.1 ± 0.976     | 55.4 ± 0.402*      | 52.5 ± 0.469*****   | 48.4 ± 3.38*****    |
| whole blood (U/g Hb)            | 161 ± 29.7    | 94.8 ± 8.35*****    | 132 ± 6*         | 129 ± 6.02**       | 111 ± 2.3***        | 106 ± 7.3***        |
| serum G6PD conc. %              | 83.4 ± 3.44   | 25.4 ± 1.14*****    | 81.8 ± 2.17      | 79 ± 1.58#         | 71 ± 1.58*****      | 67 ± 1.58*****      |

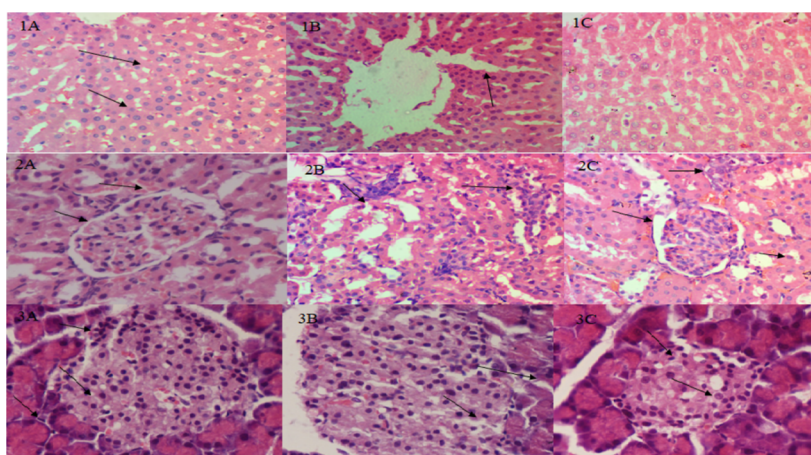


**Figure 7.** Examination of the submitted sample of liver exhibited (1A) no pathological changes. Normal hepatocytes with normal sinusoidal spaces and hepatic plates were observed (1B). Mild coagulative necrosis of hepatocytes (1C). Most hepatocytes were normal. Few hepatocytes had undergone necrotic changes. The examination of the submitted sample of kidney exhibited that (2A) proximal and distal convoluted tubules in cortical area were normal. (2B) Mild coagulative necrosis in proximal and distal convoluted tubules in cortical area and inflammation of the spaces between renal tubules, i.e., tubulointerstitial nephritis. (2C) Glomerulus were normal with intact basement membranes, Bowman's space, and Bowman's capsule. The examination of the submitted sample of pancreas exhibited that (3A) Islets of Langerhans were normal in size and insulin-producing beta cells were normal. (3B) Degenerative changes in islets of Langerhans and vacuole formation in islets of Langerhans along with mild necrosis of acinar cells of Langerhans. (3C) Islets of Langerhans were normal in size.

advised as a supplemental and alternative supplement in type 2 diabetes mellitus.

## ■ ASSOCIATED CONTENT

### SI Supporting Information

The Supporting Information is available free of charge at <https://pubs.acs.org/doi/10.1021/acsomega.3c01034>.

Impact of *C. hirsuta* Linn treatment on absorbances of DPPH, alpha amylase assays, FTIR analysis, body weight, food, water intake, blood glucose, insulin, glycosylated hemoglobin levels, biochemical analysis, relative organ weights, urine analysis, and oxidative stress markers (PDF)

## ■ AUTHOR INFORMATION

### Corresponding Author

Ali Sharif – Department of Pharmacology, Faculty of Pharmacy, The University of Lahore, Lahore 54000, Pakistan; Present Address: Department Of Pharmacology, Institute of Pharmacy, Faculty of Pharmaceutical and Allied Health Sciences, Lahore College for Women University, Lahore 54000, Pakistan; Phone: +92 345 744 066 3; Email: [alisharif.pharmacist@gmail.com](mailto:alisharif.pharmacist@gmail.com)

### Authors

Aqna Malik – Department of Pharmacology, Faculty of Pharmacy, The University of Lahore, Lahore 54000, Pakistan; [orcid.org/0000-0002-1365-3225](https://orcid.org/0000-0002-1365-3225)

Hafiz Muhammad Zubair – Department of Pharmacology, Faculty of Pharmacy, The University of Lahore, Lahore 54000, Pakistan

Bushra Akhtar – Department of Pharmacy, University of Agriculture, Faisalabad 38000, Pakistan

Aisha Mobashar – Department of Pharmacology, Faculty of Pharmacy, The University of Lahore, Lahore 54000, Pakistan

Complete contact information is available at:

<https://pubs.acs.org/10.1021/acsomega.3c01034>

### Author Contributions

A.M. performed the experimental work and participated in data interpretation. B.A. and A.M. participated in the statistical analysis. A.S. perceived the study and carried out the experimental project and data interpretation. A.S. and H.M.Z. edited the final version of the manuscript.

### Notes

The authors declare no competing financial interest. The experimental study was conducted after receiving the Animal Ethical Committee's (IREC-2018-46) clearance.

## ■ ACKNOWLEDGMENTS

The authors would like to express our heartfelt gratitude, appreciation, and thanks to Dr. Hammad Saleem for his support, advice, guidance, and words of encouragement.

## ■ REFERENCES

- (1) Hunter, P. Diet and exercise: clinical studies and molecular biology show that diet and other lifestyle changes have significant potential for treating metabolic diseases. *EMBO Rep.* **2019**, *20*, No. e47966.
- (2) Sarwar, N.; Gao, P.; Seshasai, S. R.; Gobin, R.; Kaptoge, S.; Di Angelantonio, E.; Ingelsson, E.; Lawlor, D. A.; Selvin, E.; Stampfer,

M.; et al. Diabetes mellitus, fasting blood glucose concentration, and risk of vascular disease: a collaborative meta-analysis of 102 prospective studies. *Lancet* **2010**, *375*, 2215–2222.

- (3) Bourne, R. R.; Stevens, G. A.; White, R. A.; Smith, J. L.; Flaxman, S. R.; Price, H.; Jonas, J. B.; Keeffe, J.; Leasher, J.; Naidoo, K.; et al. Causes of vision loss worldwide, 1990–2010: a systematic analysis. *Lancet Global Health* **2013**, *1*, e339–e349.

- (4) UK Prospective Diabetes Study (UKPDS) Group. Intensive blood-glucose control with sulphonylureas or insulin compared with conventional treatment and risk of complications in patients with type 2 diabetes (UKPDS 33). *Lancet* **1998**, *352*, 837–853.

- (5) Lugin, J.; Rosenblatt-Velin, N.; Parapanov, R.; Liaudet, L. The role of oxidative stress during inflammatory processes. *Biol. Chem.* **2014**, *395*, 203–230.

- (6) Chawla, R.; Chawla, A.; Jaggi, S. Microvascular and macrovascular complications in diabetes mellitus: distinct or continuum? *Indian J. Endocrinol. Metab.* **2016**, *20*, 546.

- (7) Assadi, S.; Shafiee, S. M.; Erfani, M.; Akmal, M. Antioxidative and antidiabetic effects of Capparis spinosa fruit extract on high-fat diet and low-dose streptozotocin-induced type 2 diabetic rats. *Biomed. Pharmacother.* **2021**, *138*, 111391.

- (8) Petchi, R. R.; Vijaya, C.; Parasuraman, S. J. Antidiabetic activity of polyherbal formulation in streptozotocin–nicotinamide induced diabetic Wistar rats. *J. Tradit. Complement. Med.* **2014**, *4*, 108–117.

- (9) Martinez, G. A.; Rebecchi, S.; Decorti, D.; Domingos, J. M.; Natolino, A.; Del Rio, D.; Bertin, L.; Da Porto, C.; Fava, F. Towards multi-purpose biorefinery platforms for the valorisation of red grape pomace: production of polyphenols, volatile fatty acids, polyhydroxyalkanoates and biogas. *Green Chem.* **2016**, *18*, 261–270.

- (10) Ayoola, G. A.; Ipav, S. S.; Sofidiya, M. O.; Adepoju-Bello, A. A.; Coker, H. A.; Odugbemi, T. O. Phytochemical screening and free radical scavenging activities of the fruits and leaves of *Allanblackia floribunda* Oliv (Guttiferae). *Int. J. Health Res.* **2009**, *1*, 87–93.

- (11) Luisi, G.; Stefanucci, A.; Zengin, G.; Dimmito, M. P.; Mollica, A. Anti-oxidant and tyrosinase inhibitory in vitro activity of amino acids and small peptides: New hints for the multifaceted treatment of neurologic and metabolic disfunctions. *Antioxidants* **2018**, *8*, 7.

- (12) Andargie, Y.; Sisay, W.; Molla, M.; Tessema, G. Evaluation of Antidiabetic and Antihyperlipidemic Activity of 80% Methanolic Extract of the Root of *Solanum incanum* Linnaeus (Solanaceae) in Mice. *Evid. base Compl. Alternative Med.* **2022**, *2022*, 1–12.

- (13) Torres, F. G.; Troncoso, O. P.; Vega, J.; Wong, M. Influence of botanic origin on the morphology and size of starch nanoparticles from andean native starch sources. *Polym. Renew. Resour.* **2015**, *6*, 91–103.

- (14) Abu-Reidah, I.; Contreras, M.; Arráez-Román, D.; Segura-Carretero, A.; Fernández-Gutiérrez, A. Reversed-phase ultra-high-performance liquid chromatography coupled to electrospray ionization-quadrupole-time-of-flight mass spectrometry as a powerful tool for metabolic profiling of vegetables: *Lactuca sativa* as an example of its application. *J. Chromatogr. A* **2013**, *1313*, 212–227.

- (15) Lambert, C.; Leonard, N.; De Bolle, X.; Depiereux, E. ESYPred3D: Prediction of proteins 3D structures. *Bioinformatics* **2002**, *18*, 1250–1256.

- (16) Bates, P.; Kelley, L.; MacCallum, R.; Sternberg, M. *Proteins: Struct., Funct., Bioinf.* **2001**, *45*, 39–46.

- (17) Yang, J.; Yan, R.; Roy, A.; Xu, D.; Poisson, J.; Zhang, Y. The I-TASSER Suite: protein structure and function prediction. *Nat. Methods* **2015**, *12*, 7–8.

- (18) Pieper, U.; Webb, B. M.; Dong, G. Q.; Schneidman-Duhovny, D.; Fan, H.; Kim, S. J.; Khuri, N.; Spill, Y. G.; Weinkam, P.; Hammel, M.; et al. ModBase, a database of annotated comparative protein structure models and associated resources. *Nucleic Acids Res.* **2014**, *42*, D336–D346.

- (19) Laskowski, R.; MacArthur, M.; Thornton, J. *PROCHECK: Validation of Protein-Structure Coordinates*, 2006.

- (20) Eisenberg, D.; Lüthy, R.; Bowie, J. U. [20] VERIFY3D: assessment of protein models with three-dimensional profiles. *Methods Enzymol.* **1997**, *277*, 396–404.

- (21) Gopalakrishnan, M.; Sureshkumar, P.; Thanusu, J.; Kanagarajan, V.; Govindaraju, R.; Jayasri, G. A convenient 'one-pot' synthesis and in vitro microbiological evaluation of novel 2, 7-diaryl-[1, 4]-diazepan-5-ones. *J. Enzym. Inhib. Med. Chem.* **2007**, *22*, 709–715.
- (22) Pettersen, E. F.; Goddard, T. D.; Huang, C. C.; Couch, G. S.; Greenblatt, D. M.; Meng, E. C.; Ferrin, T. E. UCSF Chimera—a visualization system for exploratory research and analysis. *J. Comput. Chem.* **2004**, *25*, 1605–1612.
- (23) Gong, Z.; Zhao, Y.; Chen, C.; Duan, Y.; Xiao, Y. Insights into ligand binding to PreQ1 riboswitch aptamer from molecular dynamics simulations. *PLoS One* **2014**, *9*, No. e92247.
- (24) Mills, N. *ChemDraw Ultra 10.0 CambridgeSoft, 100 CambridgePark Drive, Cambridge, MA 02140. www.cambridgesoft.com*. Commercial Price: 1910fordownload, 2150 for CD-ROM; Academic Price: 710fordownload, 800 for CD-ROM; ACS Publications, 2006.
- (25) Trott, O.; Olson, A. J. AutoDock Vina: improving the speed and accuracy of docking with a new scoring function, efficient optimization, and multithreading. *J. Comput. Chem.* **2010**, *31*, 455–461.
- (26) Biovia, D. *Discovery Studio Visualizer*: San Diego, CA, USA, 2017.
- (27) Thomson, M.; Al-Qattan, K. K.; Divya, J.; Ali, M. Anti-diabetic and anti-oxidant potential of aged garlic extract (AGE) in streptozotocin-induced diabetic rats. *BMC Compl. Alternative Med.* **2015**, *16*, 17.
- (28) Zhang, M.; Lv, X.-Y.; Li, J.; Xu, Z.-G.; Chen, L. The characterization of high-fat diet and multiple low-dose streptozotocin induced type 2 diabetes rat model. *Exp. Diabetes Res.* **2008**, *2008*, 1–9.
- (29) Oguanobi, N. I.; Chijioke, C. P.; Ghasi, S. Anti-diabetic effect of crude leaf extracts of *Ocimum gratissimum* in neonatal streptozotocin-induced type-2 model diabetic rats. *Int. J. Pharm. Pharmaceut. Sci.* **2012**, *4*, 77–83.
- (30) Eleazu, C.; Iroaganachi, M.; Okafor, P.; Ijeh, I.; Eleazu, K. Ameliorative potentials of ginger (*Z. officinale* Roscoe) on relative organ weights in streptozotocin induced diabetic rats. *Int. J. Biomed. Sci.* **2013**, *9*, 82.
- (31) Pan, D.; Mei, X. Antioxidant activity of an exopolysaccharide purified from *Lactococcus lactis* subsp. *lactis* 12. *Carbohydrate Polymers* **2010**, *80*, 908–914.
- (32) Rieger, J.; Pelckmann, L.-M.; Drewes, B. Preservation and Processing of Intestinal Tissue for the Assessment of Histopathology. *Animal Models of Allergic Disease*; Springer, 2021; pp 267–280.
- (33) Zhu, Y. *Microfluidic Technology for Low-Input Epigenomic Analysis*: Virginia Tech, 2018.
- (34) Singh, R. K.; Mehta, S.; Jaiswal, D.; Rai, P. K.; Watal, G. Antidiabetic effect of *Ficus bengalensis* aerial roots in experimental animals. *J. Ethnopharmacol.* **2009**, *123*, 110–114.
- (35) Chang, C. L.; Lin, Y.; Bartolome, A. P.; Chen, Y.-C.; Chiu, S.-C.; Yang, W.-C. Herbal therapies for type 2 diabetes mellitus: chemistry, biology, and potential application of selected plants and compounds. *Evidence-Based Complementary Altern. Med.* **2013**, *2013*, 378657.
- (36) (a) Zhang, B.; Jeong, J.; Burgess, B.; Jazayri, M.; Tang, Y.; Taylor Zhang, Y. Development of a rapid RP-UHPLC–MS method for analysis of modifications in therapeutic monoclonal antibodies. *J. Chromatogr., B* **2016**, *1032*, 172–181. (b) Contreras, M. d. M.; Morales-Soto, A.; Segura-Carretero, A.; Valverde, J. Potential of RP-UHPLC-DAD-MS for the qualitative and quantitative analysis of sofosbuvir in film coated tablets and profiling degradants. *J. Pharm. Biomed. Anal.* **2017**, *7*, 208–213.
- (37) Alarcon, C.; Wicksteed, B.; Prentki, M.; Corkey, B. E.; Rhodes, C. J. Succinate is a preferential metabolic stimulus-coupling signal for glucose-induced proinsulin biosynthesis translation. *Diabetes* **2002**, *51*, 2496–2504.
- (38) Xie, J.; Comeau, A. B.; Seto, C. T. Squaric acids: a new motif for designing inhibitors of protein tyrosine phosphatases. *Org. Lett.* **2004**, *6*, 83–86.
- (39) Wang, H.; Zhang, Q.; Wen, Q.; Zheng, Y.; Lazarovici, P.; Jiang, H.; Lin, J.; Zheng, W. Proline-rich Akt substrate of 40 kDa (PRAS40): a novel downstream target of PI3k/Akt signaling pathway. *Cell. Signal.* **2012**, *24*, 17–24.
- (40) Connolly, G. P.; Duley, J. A. Uridine and its nucleotides: biological actions, therapeutic potentials. *Trends Pharmacol. Sci.* **1999**, *20*, 218–225.
- (41) (a) Pandey, K. B.; Rizvi, S. I. Plant Polyphenols as Dietary Antioxidants in Human Health and Disease. *Oxid. Med. Cell. Longev.* **2009**, *2*, 270–278. (b) Wu, L.; Hafiz, M. Z.; Guan, Y.; He, S.; Xiong, J.; Liu, W.; Yan, B.; Li, X.; Yang, J. 17 $\beta$ -estradiol suppresses carboxylesterases by activating c-Jun/AP-1 pathway in primary human and mouse hepatocytes. *Eur. J. Pharmacol.* **2018**, *819*, 98–107.
- (42) Grant, J.; Ryland, D.; Isaak, C. K.; Prashar, S.; Siow, Y. L.; Taylor, C. G.; Aliani, M. Effect of Vitamin D<sub>3</sub> Fortification and Saskatoon Berry Syrup Addition on the Flavor Profile, Acceptability, and Antioxidant Properties of Rooibos Tea (*Aspalathus linearis*). *J. Food Sci.* **2017**, *82*, 807–817.
- (43) Yibchok-anun, S.; Abu-Basha, E. A.; Yao, C.-Y.; Panichkriangkrai, W.; Hsu, W. H. The role of arginine vasopressin in diabetes-associated increase in glucagon secretion. *Regul. Pept.* **2004**, *122*, 157–162.
- (44) Berteau, M.; Rütli, M. F.; Othman, A.; Marti-Jaun, J.; Hersberger, M.; von Eckardstein, A.; Hornemann, T. Deoxysphingoid bases as plasma markers in diabetes mellitus. *Lipids Health Dis.* **2010**, *9*, 84–87.
- (45) Muccee, F.; Ejaz, S.; Riaz, N. Toluene degradation via a unique metabolic route in indigenous bacterial species. *Arch. Microbiol.* **2019**, *201*, 1369–1383.
- (46) Nagano, T.; Fridovich, I. Superoxide radical from xanthine oxidase acting upon lumazine. *J. Free Radic. Biol. Med.* **1985**, *1*, 39–42.
- (47) (a) Basumatary, S.; Narzary, H. Nutritional value, phytochemicals and antioxidant property of six wild edible plants consumed by the Bodos of North-East India. *Mediterr. J. Nutr. Metabol.* **2017**, *10*, 259–271. (b) Narzary, H.; Islary, A.; Basumatary, S. Study of antimicrobial properties of six wild vegetables of medicinal value consumed by the Bodos of Assam, India. *Medicinal Plants—International Journal of Phytomedicines and Related Industries* **2018**, *10*, 363–368.
- (48) (a) Rajan, T.; Muthukrishnana, S. Characterization of phenolic compounds in *Pseudarthria viscidra* root extract by HPLC and FT-IR analysis. *Asian J. Pharmaceut. Clin. Res.* **2013**, *6*, 274–276. (b) Kang, Y.-F.; Liu, C.-M.; Kao, C.-L.; Chen, C.-Y. Antioxidant and anticancer constituents from the leaves of *Liriodendron tulipifera*. *Molecules* **2014**, *19*, 4234–4245. (c) Domínguez-Martínez, I.; Meza-Márquez, O. G.; Osorio-Revilla, G.; Proal-Nájera, J.; Gallardo-Velázquez, T. Determination of capsaicin, ascorbic acid, total phenolic compounds and antioxidant activity of *Capsicum annuum* L. var. *serrano* by mid infrared spectroscopy (Mid-FTIR) and chemometric analysis. *Appl. Biol. Chem.* **2014**, *57*, 133–142. (d) Oliveira, R. N.; Mancini, M. C.; Oliveira, F. C. S. d.; Passos, T. M.; Quilty, B.; Thiré, R. M. d. S. M.; McGuinness, G. B. FTIR analysis and quantification of phenols and flavonoids of five commercially available plants extracts used in wound healing. *Materia* **2016**, *21*, 767–779.
- (49) Hsu, W.-H.; Lu, S.-S.; Lee, B.-H.; Hsu, Y.-W.; Pan, T.-M. Monacolin K and monascin attenuated pancreas impairment and hyperglycemia induced by advanced glycation endproducts in BALB/c mice. *Food Funct.* **2013**, *4*, 1742–1750.
- (50) Liao, Z.; Chen, X.; Wu, M. Antidiabetic effect of flavones from *Cirsium japonicum* DC in diabetic rats. *Arch. Pharm. Res.* **2010**, *33*, 353–362.
- (51) Singh, A. B.; Singh, N.; Maurya, R.; Srivastava, A. K. Anti-hyperglycaemic, lipid lowering and anti-oxidant properties of [6]-gingerol in db/db mice. *Int. J. Med. Med. Sci.* **2009**, *1*, 536–544.

(52) Phoebe Chen, Y.-P.; Chen, F. Identifying targets for drug discovery using bioinformatics. *Expert Opin. Ther. Targets* **2008**, *12*, 383–389.

(53) Bleicher, K. H.; Böhm, H.-J.; Müller, K.; Alanine, A. I. Hit and lead generation: beyond high-throughput screening. *Nat. Rev. Drug Discov.* **2003**, *2*, 369–378.

(54) Chen, Y.; Liu, L. Modern methods for delivery of drugs across the blood–brain barrier. *Adv. Drug Deliv. Rev.* **2012**, *64*, 640–665.

(55) Dimitrov, S.; Pavlov, T.; Nedelcheva, D.; Reuschenbach, P.; Silvani, M.; Bias, R.; Comber, M.; Low, L.; Lee, C.; Parkerton, T.; et al. A kinetic model for predicting biodegradation. *SAR QSAR Environ. Res.* **2007**, *18*, 443–457.

(56) Kandemir, F. M.; Ozkaraca, M.; Küçükler, S.; Caglayan, C.; Hanedan, B. Preventive effects of hesperidin on diabetic nephropathy induced by streptozotocin via modulating TGF- $\beta$ 1 and oxidative DNA damage. *Toxin Rev.* **2018**, *37*, 287–293.

(57) Panichayupakaranant, P.; Shah, M.; Muhammad, H.; Mehmood, Y.; Khalil, R.; Ul-Haq, Z. Superoxide scavenging and antiglycation activity of rhinacanthins-rich extract obtained from the leaves of *Rhinacanthus nasutus*. *Pharmacogn. Mag.* **2017**, *13*, 652.

(58) Muthumani, M.; Miltonprabu, S. Ameliorative efficacy of tetrahydrocurcumin against arsenic induced oxidative damage, dyslipidemia and hepatic mitochondrial toxicity in rats. *Chem. Biol. Interact.* **2015**, *235*, 95–105.

(59) Zafar, M.; Naeem-ul-Hassan Naqvi, S. Effects of STZ-induced diabetes on the relative weights of kidney, liver and pancreas in albino rats: a comparative study. *Int. J. Morphol.* **2010**, *28*, 135.

(60) (a) Jadhav, R.; Puchchakayala, G. Hypoglycemic and antidiabetic activity of flavonoids: boswellic acid, ellagic acid, quercetin, rutin on streptozotocin-nicotinamide induced type 2 diabetic rats. *Chemistry* **2012**, *1*, 100g. (b) Torres-Piedra, M.; Ortiz-Andrade, R.; Villalobos-Molina, R.; Singh, N.; Medina-Franco, J. L.; Webster, S. P.; Binnie, M.; Navarrete-Vázquez, G.; Estrada-Soto, S. A comparative study of flavonoid analogues on streptozotocin–nicotinamide induced diabetic rats: Quercetin as a potential antidiabetic agent acting via 11 $\beta$ -Hydroxysteroid dehydrogenase type 1 inhibition. *Eur. J. Med. Chem.* **2010**, *45*, 2606–2612.

(61) Fawzi Mahomoodally, M.; Mollica, A.; Stefanucci, A.; Zakariyyah Aumeeruddy, M.; Poorneeka, R.; Zengin, G. Volatile components, pharmacological profile, and computational studies of essential oil from *Aegle marmelos* (Bael) leaves: A functional approach. *Ind. Crop. Prod.* **2018**, *126*, 13–21.

(62) Kirkwood, T. B.; Kowald, A. The free-radical theory of ageing—older, wiser and still alive: modelling positional effects of the primary targets of ROS reveals new support. *Bioessays* **2012**, *34*, 692–700.

(63) Ashraf, H.; Heidari, R.; Nejati, V.; Ilkhanipoor, M. Aqueous extract of *Berberis integerrima* root improves renal dysfunction in streptozotocin induced diabetic rats. *Avicenna J. Phytomed.* **2013**, *3*, 82.